Inorganic Chemistry

Article

Unusual Structural Types in Polynuclear Iron Chemistry from the Use of *N*,*N*,*N′*,*N′*-Tetrakis(2-hydroxyethyl)ethylenediamine (edteH₄): Fe₅, Fe₆, and Fe₁₂ Clusters

Rashmi Bagai, Matthew R. Daniels, Khalil A. Abboud, and George Christou*

Department of Chemistry, University of Florida, Gainesville, Florida 32611-7200

Received December 12, 2007

The syntheses, crystal structures, and magnetochemical characterization of five new iron clusters $[Fe_5O_2(O_2CPh)_7(edte)(H_2O)]$ (**1**), $[Fe_6O_2(O_2CBu^t)_8(edteH)_2]$ (**2**), $[Fe_{12}O_4(OH)_2(O_2CMe)_6(edte)_4(H_2O)_2](ClO_4)_4$ (**3**), $[Fe_{12}O_4(OH)_8(edte)_4(H_2O)_2](ClO_4)_4$ (**4**), and $[Fe_{12}O_4(OH)_8(edte)_4(H_2O)_2](NO_3)_4$ (**5**) (edteH₄ = $N,N,N′,N′$-tetrakis(2-hydroxyethyl)ethylenediamine) are reported. The reaction of edteH₄ with $[Fe_3O(O_2CPh)_6(H_2O)_3](NO_3)$ and $[Fe_3O(O_2CBu^t)_6(H_2O)_3](OH)$ gave **1** and **2**, respectively. Complex **3** was obtained from the reaction of edteH₄ and NaO₂CMe with $Fe(ClO_4)_3$, whereas **4** and **5** were obtained from the reaction of edteH₄ with $Fe(ClO_4)_3$ and $Fe(NO_3)_3$, respectively. The core of **1** consists of a $[Fe_4(\mu_3\text{-}O)_2]^{8+}$ butterfly unit to which is attached a fifth Fe atom by four bridging O atoms. The core of **2** consists of two triangular $[Fe_3(\mu_3\text{-}O)]^{7+}$ units linked together by six bridging O atoms. Finally, the cores of **3**−**5** consist of an $[Fe_{12}(\mu_4\text{-}O)_4(\mu\text{-}OH)_2]^{26+}$ unit. Variable-temperature (*T*) and -field (*H*) solid-state direct and alternating current magnetization (*M*) studies were carried out on complexes **1**−**3** in the 1.8–300 K range. Analysis of the obtained data revealed that **1**, **2**, and **3**−**5** possess an *S* = 5/2, 5, and 0 ground-state spin, respectively. The fitting of the obtained $M/N\mu_B$ vs *H/T* data was carried out by matrix diagonalization, and this gave values for the axial zero-field splitting (ZFS) parameter *D* of −0.50 cm⁻¹ for **1** and –0.28 cm⁻¹ for **2**.

Introduction

Polynuclear Fe(III) compounds with O and N based ligation are of interest primarily because of their relevance in bioinorganic chemistry and single-molecule magnetism.[1] Owing to the high charge-to-size ratio of Fe(III) and the resulting propensity to favor oxide bridges, high nuclearity species are often encountered in Fe(III) chemistry,[2] and these have also been of interest as models of intermediate stages of the build-up of the giant Fe/O core protein ferritin, the Fe storage protein in most living mammalian life.[3] In addition, if the nuclearity of polynuclear Fe(III) clusters is large enough and if the clusters also possess the appropriate Fe_x topologies, then they can sometimes possess large ground-state spin (*S*) values as a result of spin frustration

effects among the various Fe_2 pairwise exchange pathways, even though these exchange interactions are essentially always antiferromagnetic.[4]

For the above reasons and more, we continue to seek new synthetic methods to new Fe_x complexes. We have recently been exploring various polydentate chelate groups that can also function as bridging groups and which can thus foster formation of high nuclearity products. As part of this work, we have most recently been investigating chelating/bridging groups with an ethylenediamine backbone. We recently reported, for example, the use of deprotonated dmemH and heenH₂ (Scheme 1) as new and flexible N,N,O and O,N,N,O chelates, respectively, for the synthesis of Fe₃, Fe₆, Fe₇, Fe₉ and Fe₁₈ complexes.[5] In addition to unusual Fe_x topologies in some of these complexes, Fe₁₈ represents the highest-nuclearity chain-like metal-containing molecule to be yet discovered, and Fe₉ contains a mixture of ON and OFF dimers with respect to quantum mechanical coupling through the hydrogen bond. The deprotonated hydroxyethyl arms of such chelates are excellent bridging groups and favor the formation of high nuclearity species from these reactions. In the present work, we have extended this study by

---

* To whom correspondence should be addressed. E-mail: christou@chem.ufl.edu. Phone: +1-352-392-8314. Fax: +1-352-392-8757.

(1) (a) Bertini, I.; Gray, H. B.; Lippard, S. J.; Valentine, J. S. *Bioinorganic Chemistry*; University Science Books: Mill Valley, CA, 1994. (b) Gatteschi, D.; Sessoli, R.; Cornia, A. *Chem. Commun.* **2000**, 725. (c) Christou, G.; Gatteschi, D.; Hendrickson, D. N.; Sessoli, R. *MRS Bull.* **2000**, *25*, 66. (d) Aromi, G.; Brechin, E. K. *Struct. Bonding (Berlin)* **2006**, *122*, 1.

Scheme 1
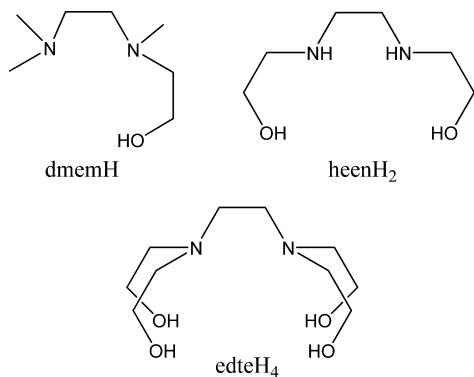
exploring a related, potentially hexadentate ligand *N,N,N′,N′*-tetrakis(2-hydroxyethyl)ethylenediamine (edteH₄; Scheme 1), which provides four potentially bridging hydroxyethyl arms on an ethylenediamine backbone. There are no literature reports of any polynuclear Fe complex with deprotonated edteH₄, but it was considered likely that many such species were awaiting discovery. One reason for believing that edteH₄ is an attractive potential route to new Fe$_x$ clusters was our very recent investigations with edteH₄ in Mn chemistry, where we obtained Mn₈, Mn₁₂, and Mn₂₀ complexes with new core topologies distinctly different from any seen previously.[6a] One of these products was also reported at the same time by another group.[6b] We have now found that the use of edteH₄ in Fe chemistry also leads to interesting new structural types of products. We herein report the syntheses, structures and magnetochemical properties of the obtained Fe₅, Fe₆, and Fe₁₂ complexes.

Experimental Section

Syntheses. All preparations were performed under aerobic conditions using reagents and solvents as received. [Fe₃O-(O₂CPh)₆(H₂O)₃](NO₃) and [Fe₃O(O₂CBu^t)₆(H₂O)₃](OH) was synthesized as reported elsewhere.[7]

[Fe₅O₂(O₂CPh)₇(edte)(H₂O)] (1). To a stirred solution of edteH₄ (0.05 g, 0.21 mmol) in CH₂Cl₂ (15 mL) was added [Fe₃O(O₂CPh)₆-(H₂O)₃](NO₃)(0.38 g, 0.37 mmol). The mixture was stirred for 30 min, filtered to remove undissolved solid, and the filtrate layered with a 1:1 (v/v) mixture of Et₂O and hexanes. X-ray quality orange crystals of **1**·CH₂Cl₂ slowly formed over a period of 5 days. These were collected by filtration, washed with Et₂O, and dried in vacuo. The yield was 20%. Anal. Calc (Found) for **1** (C₅₉H₅₇N₂Fe₅O₂₁): C, 50.28 (50.63); H, 4.07 (4.27); N, 1.99 (1.85). Selected IR data (cm⁻¹): 2862 (w), 1597 (m), 1552 (s), 1534 (s), 1400 (s), 1175 (w), 1087 (m), 1067 (m), 1024 (w), 928 (w), 892 (w), 863 (w), 720 (s), 653 (m), 602 (w), 529 (w), 465 (m).

[Fe₆O₂(O₂CBu^t)₈(edteH)₂] (2). To a stirred solution of edteH₄ (0.10 g, 0.42 mmol) in CHCl₃ (15 mL) was added [Fe₃O(O₂CBu^t)₆-(H₂O)₃](OH) (0.18 g, 0.21 mmol). The mixture was stirred for 30 min, filtered to remove undissolved solid, and the filtrate layered with pentanes. X-ray quality orange crystals of **2**·2CHCl₃ slowly formed over a week. These were collected by filtration, washed with pentanes, and dried in vacuo. The yield was 10%. The dried solid appeared to be very hygroscopic, analyzing as the tetrahydrate. Anal. Calc (Found) for **2**·2CHCl₃·4H₂O (C₆₂H₁₂₄N₄Fe₆Cl₆O₃₀): C, 38.12 (37.98); H, 6.40 (6.33); N, 2.87 (3.24). Selected IR data (cm⁻¹): 2960 (m), 2869 (m), 1562 (s), 1483 (s), 1421 (s), 1375 (m), 1360 (m), 1227 (m), 1098 (m), 1042 (w), 909 (w), 788 (w), 694 (m), 603 (m), 554 (m), 480 (w), 429 (m).

[Fe₁₂O₄(OH)₂(O₂CMe)₆(edte)₄(H₂O)₂](ClO₄)₄ (3). To a stirred solution of edteH₄ (0.10 g, 0.42 mmol) in MeCN (15 mL) was added NaO₂CMe·3H₂O (0.23 g, 1.69 mmol) followed by Fe(ClO₄)₃·6H₂O (0.39 g, 0.85 mmol). The mixture was stirred for 30 min, filtered to remove undissolved solid, and the filtrate left to slowly concentrate by evaporation. X-ray quality orange crystals of **3**·4MeCN slowly formed over a week. These were collected by filtration, washed with MeCN, and dried in vacuo. The yield was 40%. Anal. Calc (Found) for **3** (C₅₂H₁₀₄N₈Fe₁₂Cl₄O₅₂): C, 25.13 (24.82); H, 4.22 (4.21); N, 4.51 (4.47). Selected IR data (cm⁻¹):

(2) (a) Smith, A. A.; Coxall, R. A.; Harrison, A.; Helliwell, M.; Parsons, S.; Winpenny, R. E. P. *Polyhedron* **2004**, *23*, 1557. (b) Canada-Vilalta, C.; Pink, M.; Christou, G. *Chem.Commun.* **2003**, 1240. (c) Tolis, E. I.; Helliwell, M.; Langley, S.; Raftery, J.; Winpenny, R. E. P. *Angew. Chem., Int. Ed.* **2003**, *42*, 3804. (d) Glaser, T.; Lugger, T.; Hoffmann, R. D. *Eur. J. Inorg. Chem.* **2004**, 2356. (e) Frey, M.; Harris, S. G.; Holmes, J. M.; Nation, D. A.; Parsons, S.; Tasker, P. A.; Teat, S. J.; Winpenny, R. E. P. *Angew. Chem., Int. Ed.* **1998**, *37*, 3246. (f) Frey, M.; Harris, S. G.; Holmes, J. M.; Nation, D. A.; Parsons, S.; Tasker, P. A.; Winpenny, R. E. P. *Chem.—Eur. J.* **2000**, *6*, 1407. (g) Abbati, G. L.; Caneschi, A.; Cornia, A.; Fabretti, A. C.; Gatteschi, D. *Inorg. Chim. Acta* **2000**, *297*, 291. (h) Caneschi, A.; Cornia, A.; Fabretti, A. C.; Gatteschi, D. *Angew. Chem., Int. Ed. Engl.* **1995**, *34*, 2716. (i) Heath, S. L.; Powell, A. K. *Angew. Chem., Int. Ed. Engl.* **1992**, *31*, 191. (j) Jones, L. F.; Batsanov, A.; Brechin, E. K.; Collison, D.; Helliwell, M.; Mallah, T.; McInnes, E. J. L.; Piligkos, S. *Angew. Chem., Int. Ed.* **2002**, *41*, 4318. (k) Belli Dell'Amico, D.; Boschi, D.; Calderazzo, F.; Ianelli, S.; Labella, L.; Marchetti, F.; Pelizzi, G.; Quadrelli, E. G. F. *Inorg. Chim. Acta* **2000**, *300*, 882. (l) Asirvatham, S.; Khan, M. A.; Nicholas, K. M. *Inorg. Chem.* **2000**, *39*, 2006. (m) Micklitz, W.; Lippard, S. J. *J. Am. Chem. Soc.* **1989**, *111*, 6856. (n) Caneschi, A.; Cornia, A.; Lippard, S. J.; Papaefthymiou, G. C.; Sessoli, R. *Inorg. Chim. Acta* **1996**, *243*, 295. (o) Low, D. M.; Jones, L. F.; Bell, A.; Brechin, E. K.; Mallah, T.; Riviere, E.; Teat, S. J.; McInnes, E. J. L. *Angew. Chem., Int. Ed.* **2003**, *42*, 3781. (p) Bino, A.; Ardon, M.; Lee, D.; Spingler, B.; Lippard, S. J. *J. Am. Chem. Soc.* **2002**, *124*, 4578. (q) Taft, K. L.; Papaefthymiou, G. C.; Lippard, S. J. *Inorg. Chem.* **1994**, *33*, 1510.

(3) (a) Taft, K. L.; Papaefthymiou, G. C.; Lippard, S. J. *Science* **1993**, *259*, 1302. (b) Gorun, S. M.; Papaefthymiou, G. C.; Frankel, R. B.; Lippard, S. J. *J. Am. Chem. Soc.* **1987**, *109*, 3337. (c) Kurtz, D. M., Jr. *Chem Rev* **1990**, *90*, 585.

(4) (a) Powell, A. K.; Heath, S. L.; Gatteschi, D.; Pardi, L.; Sessoli, R.; Spina, G.; Del Giallo, F.; Pieralli, F. *J. Am. Chem. Soc.* **1995**, *117*, 2491. (b) Goodwin, J. C.; Sessoli, R.; Gatteschi, D.; Wernsdorfer, W.; Powell, A. K.; Heath, S. L. *Dalton Trans.* **2000**, 1835. (c) Barra, A. L.; Caneschi, A.; Cornia, A.; de Biani, F. F.; Gatteschi, D.; Sangregorio, C.; Sessoli, R.; Sorace, L. *J. Am. Chem. Soc.* **1999**, *121*, 5302. (d) Powell, G. W.; Lancashire, H. N.; Brechin, E. K.; Collison, D.; Health, S. L.; Malluh, T.; Wernsdorfer, W. *Angew. Chem., Int. Ed.* **2004**, *43*, 5772. (e) Schmitt, W.; Anson, C. E.; Wernsdorfer, W.; Powell, A. K. *Chem. Commun.* **2005**, 2098. (f) Moragues-Canovas, M.; Riviere, P.; Ricard, L.; Paulsen, C.; Wernsdorfer, W.; Rajaraman, G.; Brechin, E. K.; Mallah, T. *Adv. Mater.* **2004**, *16*, 1101. (g) Kajiwara, T.; Ito, T. *Angew. Chem., Int. Ed.* **2000**, *39*, 230. (h) Jones, L. F.; Brechin, E. K.; Collison, D.; Helliwell, M.; Mallah, T.; Piligkos, S.; Rajaraman, G.; Wernsdorfer, W. *Inorg. Chem.* **2003**, *42*, 6601. (i) Delfs, C.; Gatteschi, D.; Pardi, L.; Sessoli, R.; Wieghardt, K.; Hanke, D. *Inorg. Chem.* **1993**, *32*, 3099.

(5) (a) Bagai, R.; Datta, S.; Betancur-Rodriguez, A.; Abboud, K. A.; Hill, S.; Christou, G. *Inorg. Chem.* **2007**, *46*, 4535. (b) Bagai, R.; Abboud, K. A.; Christou, G. *Chem. Commun.* **2007**, 3359. (c) Bagai, R.; Wernsdorfer, W.; Abboud, K. A.; Christou, G. *J. Am. Chem. Soc.* **2007**, *129*, 12918.

(6) (a) Bagai, R.; Abboud, K. A.; Christou, G. *Inorg. Chem.* **2008**, *47*, 621. (b) Zhou, A. J.; Qin, L. J.; Beedle, C. C.; Ding, S.; Nakano, M.; Leng, J. D.; Tong, M. L.; Hendrickson, D. N. *Inorg. Chem.* **2007**, *46*, 8111.

(7) (a) Duncan, J. F.; Kanekar, C. R.; Mok, K. F. *J. Chem. Soc. A* **1969**, *3*, 480. (b) Earnshaw, A.; Figgis, B. N.; Lewis, J. *J. Chem. Soc. A* **1966**, *12*, 1656. (c) Wu, R. W.; Poyraz, M.; Sowrey, F. E.; Anson, C. E.; Wocadlo, S.; Powell, A. K.; Jayasooriya, U. A.; Cannon, R. D.; Nakamoto, T.; Katada, M.; Sano, H. *Inorg. Chem.* **1998**, *37*, 1913.

2884 (m), 1559 (s), 1455 (s), 1336 (w), 1271 (w), 1086 (s), 933 (m), 904 (m), 744 (w), 624 (s), 532 (m), 466 (w), 437 (w).

[Fe₁₂O₄(OH)₈(edte)₄(H₂O)₂](ClO₄)₄ (4). To a stirred solution of edteH₄ (0.05 g, 0.21 mmol) in EtOH (15 mL) was added Fe(ClO₄)₃·6H₂O (0.39 g, 0.85 mmol). The mixture was stirred for 30 min, filtered to remove undissolved solid, and the filtrate left to slowly concentrate by evaporation. X-ray quality orange crystals of **4** slowly formed over a week. These were collected by filtration, washed with EtOH, and dried in vacuo. The yield was 20%. Anal. Calc (Found) for **4** (C₄₀H₉₂N₈Fe₁₂Cl₄O₄₆): C, 21.66 (21.51); H, 3.74 (4.15); N, 5.31 (5.02). Selected IR data (cm⁻¹): 2867 (m), 1628 (w), 1469 (w), 1363 (w), 1270 (w), 1088 (s), 935 (m), 910 (m), 740 (w), 661 (m), 627 (s), 583 (w), 490 (m).

[Fe₁₂O₄(OH)₈(edte)₄(H₂O)₂](NO₃)₄ (5). To a stirred solution of edteH₄ (0.10 g, 0.42 mmol) in MeOH (15 mL) was added NEt₃ (0.12 mL, 0.85 mmol) followed by Fe(NO₃)₃·9H₂O (0.34 g, 0.85 mmol). The mixture was stirred for 30 min, and filtered to remove undissolved solid. Vapor diffusion of THF into the filtrate gave needle-like orange crystals of **5**. These were collected by filtration, washed with THF, and dried in vacuo. The yield was 10%. Anal. Calc (Found) for **5** (C₄₀H₉₂N₁₂Fe₁₂O₄₂): C, 23.29 (23.06); H, 4.61 (4.45); N, 8.12 (8.07). Selected IR data (cm⁻¹): 2938 (w), 2677 (m), 1650 (w), 1385 (s), 1171 (w), 1057 (m), 934 (m), 909 (m), 825 (m), 636 (m), 613 (w), 525 (w), 492 (m).

X-ray Crystallography. Data were collected at 173 K on a Siemens SMART PLATFORM equipped with a CCD area detector and a graphite monochromator utilizing Mo Kα radiation (λ = 0.71073 Å). Suitable crystals of **1**·CH₂Cl₂, **2**·2CHCl₃, **3**·4MeCN, and **4** were attached to glass fibers using silicone grease and transferred to a goniostat where they were cooled to 173 K for data collection. Cell parameters were refined using up to 8192 reflections. A full sphere of data (1850 frames) was collected using the ω-scan method (0.3° frame width). The first 50 frames were remeasured at the end of the data collection to monitor the instrument and the crystal stability (maximum correction on I was <1%). Absorption corrections by integration were applied based on measured indexed crystal faces. The structure was solved by direct methods in SHELXTL6,[8] and refined on F^2 using full-matrix least-squares. The non-H atoms were treated anisotropically, whereas the hydrogen atoms were placed in calculated, ideal positions, and included in the refinement as riding on their respective carbon atoms.

For **2**·2CHCl₃, the asymmetric unit consists of half-an Fe₆ cluster and a CHCl₃ molecule. Two Buᵗ groups are disordered and were refined in two parts each. A total of 481 parameters were refined in the final cycle of refinement using 6037 reflections with I > $2\sigma(I)$ to yield R_1 and wR_2 of 5.75 and 13.64%, respectively.

For **3**·4MeCN, the asymmetric unit consists of the Fe₁₂ cluster, three whole and two half-perchlorate anions, which are all disordered, and four MeCN molecules, three of which are very disordered. The program SQUEEZE,[9] a part of the PLATON package of crystallographic software, was used to calculate the solvent disorder area and remove its contribution to the overall intensity data. The N9 MeCN molecule was not removed by SQUEEZE[9] because it is hydrogen-bonded to the O17−H17 hydroxyl group and not disordered. The Cl1 perchlorate is hydrogen-bonded to the opposite hydroxyl group (O17−H17) through O38. While each disordered perchlorate anion was refined in two parts, the second part of the Cl3 (Cl3′) was not complete, only one O atom being located. The charges are balanced by the fact that the groups occupying the O5 and O27 positions represent

a disorder between a water molecule and a carboxyl group. The others could not be found because of the heavy disorder. Finally, the hydroxyl protons and the coordinated water protons were obtained from a difference Fourier map and included as riding on their parent O atoms. A total of 1165 parameters were refined in the final cycle of refinement using 10158 reflections with I > $2\sigma(I)$ to yield R_1 and wR_2 of 7.88 and 22.19%, respectively.

Severe disorder problems were encountered for **1**·CH₂Cl₂ and **4**. For **1**·CH₂Cl₂, the asymmetric unit consists of an Fe₅ cluster and a dichloromethane molecule; the structure exhibited much disorder in the benzoate phenyl rings and the edte⁴⁻ groups, preventing satisfactory refinement of the structure. However, the core was well observed and showed no disorder. For **4**, the asymmetric unit consists of half an Fe₁₂ cluster and two perchlorate anions; again, the structure exhibited bad disorder among the peripheral ligands. Despite examination of many crystals of both compounds, we could not find ones that diffracted well enough to allow data of sufficient quantity and quality to be obtained for satisfactory structure refinement. Thus, the structures were refined as far as possible so that we could at least identify the overall structure and nuclearity of the complexes for comparison with **2** and **3**, which we were able to do successfully. Knowing the number and arrangement of the Fe atoms in the core was also essential for the interpretation of the magnetic data of **1** and **4**. We include and briefly describe the structures of these two complexes in this paper only for the mentioned purposes; the metric parameters are unreliable and are not discussed. Unit cell data and details of the structure refinements for complexes **1−4** are listed in Table 1.

Other Studies. IR spectra were recorded in the solid state (KBr pellets) on a Nicolet Nexus 670 FTIR spectrometer in the 400–4000 cm⁻¹ range. Elemental analyses (C, H, and N) were performed by the in-house facilities of the University of Florida Chemistry Department. Variable-temperature direct current (dc) and alternating current (ac) magnetic susceptibility data were collected at the University of Florida using a Quantum Design MPMS-XL SQUID susceptometer equipped with a 7 T magnet and operating in the 1.8–300 K range. Samples were embedded in solid eicosane to prevent torquing. Magnetization versus field and temperature data were fit using the program MAGNET.[10] Experimental data were corrected for the diamagnetism of the sample holder and for the diamagnetic contributions of the samples, the latter calculated from Pascal's constants.[11] These were subtracted from the experimental susceptibility to give the molar paramagnetic susceptibility (χ_M).

Results and Discussion

Syntheses. A variety of reactions of edteH₄ were explored with a number of different Fe(III) starting materials and under different reagent ratios, solvents, and other conditions before the following successful procedures were identified. The reaction of [Fe₃O(O₂CPh)₆(H₂O)₃](NO₃) with edteH₄ in a ~3:2 molar ratio in CH₂Cl₂ followed by layering with Et₂O−hexanes (1:1 v/v) gave orange needle-like crystals of [Fe₅O₂(O₂CPh)₇(edte)(H₂O)] (**1**). Its formation is summarized in eq 1.

(8) *SHELXTL*; Bruker-AXS: Madison, WI, 2000.
(9) Vandersluis, P.; Spek, A. L. *Acta Crystallogr., Sect. A* **1990**, *46*, 194.
(10) Davidson, E. R. *MAGNET*; Indiana University: Bloomington, IN, 1999.
(11) *CRC Handook of Chemistry and Physics*, 64th ed.; Weast, R. C., Ed.; CRC Press: Boca Raton, FL, 1984.

$$5[Fe_3O(O_2CPh)_6(H_2O)_3]^+ + 3edteH_4 \rightarrow$$
$$3[Fe_5O_2(O_2CPh)_7(edte)(H_2O)] +$$
$$9PhCO_2H + 11H_2O + 5H^+ \quad (1)$$
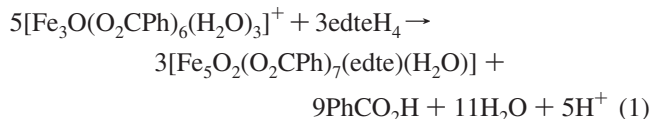
The benzoate groups clearly function as proton acceptors facilitating the deprotonation of edteH₄ in the absence of added base. In this and the procedures to follow, the nonoptimized yields of product are relatively low, but reproducible, and we were happy to sacrifice yield in exchange for pure, highly crystalline material. The filtrates were still colored, but we did not pursue further product isolation by, for example, addition of a cosolvent. With other chelates such as dmemH,[5a] we have found that the identity of the Fe$_x$ product depends on the carboxylate employed,[5a] and thus we also explored reactions of edteH₄ with other $[Fe_3O(O_2CR)_6(H_2O)_3]^+$ reagents. With pivalate (R = Bu^t), a related reaction to that which gave **1**, but with a $[Fe_3O(O_2CBu^t)_6(H_2O)_3]^+$ to edteH₄ molar ratio of 1:2 in CHCl₃, gave a brown solution and subsequent isolation of $[Fe_6O_2(O_2CBu^t)_8(edteH)_2]$ (**2**) on layering with pentanes. The proton acceptors in this reaction are the carboxylate groups and the OH⁻ anions; the formation of **2** is summarized in eq 2.

$$2[Fe_3O(O_2CBu^t)_6(H_2O)_3](OH) + 2edteH_4 \rightarrow$$
$$[Fe_6O_2(O_2CBu^t)_8(edteH)_2] + 4Bu^tCO_2H + 8H_2O \quad (2)$$
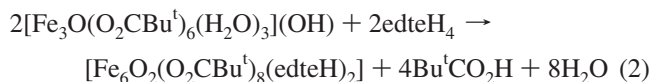
The same product was also obtained using CH₂Cl₂ as the solvent but in poor crystallinity and decreased yield.

We also explored the use of simple Fe(III) salts as reagents, in the presence of added carboxylate groups as proton acceptors. The reaction of Fe(ClO₄)₃·6H₂O with edteH₄ and NaO₂CMe·3H₂O in a 2:1:4 ratio in MeCN gave a brown solution from which was obtained $[Fe_{12}O_4(OH)_2(edte)_4$-$(O_2CMe)_6(H_2O)_2](ClO_4)_4$ (**3**). Its preparation is summarized in eq 3.

$$12Fe^{3+} + 32MeCO_2^- + 4edteH_4 + 8H_2O \rightarrow$$
$$[Fe_{12}O_4(OH)_2(edte)_4(O_2CMe)_6(H_2O)_2]^{4+} + 26MeCO_2H \quad (3)$$
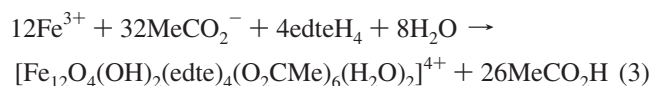
Decreasing the amount of acetate from 4 to 2 equiv drastically reduced the reaction yield, as expected from eq 3. Complex **3** was also obtained from a MeCN:MeOH

solvent system. However, when the reaction of Fe(ClO₄)₃·6H₂O with edteH₄ in a 4:1 ratio was carried out in neat EtOH in the absence of NaO₂CMe, the product was $[Fe_{12}O_4(OH)_8(edte)_4(H_2O)_2](ClO_4)_4$ (**4**), obtained as orange needles on layering the solution with CHCl₃. Complex **4** is structurally very similar to **3**, except that the acetate groups have been replaced by hydroxide ions (vide infra). In a related fashion, the reaction of Fe(NO₃)₃ with edteH₄ and NEt₃ in a 2:1:2 ratio in MeOH gave $[Fe_{12}O_4(OH)_8(edte)_4$-$(H_2O)_2](NO_3)_4$ (**5**) on vapor diffusion with tetrahydrofuran; the product was identified by elemental analysis and IR and magnetic comparisons with complexes **3** and **4** (vide infra). When the reaction was carried out in EtOH, as for **4**, no clean product could be isolated. The yield of **5** was much lower than that of **4**, presumably because of the solubility of the product, although it could be somewhat improved by addition of some NEt₃ to the reaction.

It is clear that the reactions that lead to **1**−**5** are very complicated and involve acid/base and redox chemistry, as well as structural fragmentations and rearrangements, and the reaction solutions likely contain a complicated mixture of several species in equilibrium. As is usually the case in such reaction systems, the identity of the products is sensitive to various factors such as the relative solubilities of species in equilibrium and the crystallization kinetics, and this rationalizes the fact that changing the carboxylate from benzoate to acetate causes a major change in the isolated product, from Fe₅ to Fe₁₂.

Description of Structures. A labeled representation of the partially refined structure of $[Fe_5O_2(O_2CPh)_7(edte)(H_2O)]$ (**1**) is shown in Figure 1. While we would not normally report structures that could not be fully refined, in this case knowledge of the core nuclearity and topology are essential for proper interpretation of the magnetic properties of **1** (and **4** and **5**), and for their comparison with the structures and magnetic properties of **2** and **3**. We thus provide only a minimum discussion of the core connectivity and ligand binding modes.

Table 1. Crystallographic Data for **1**·CH₂Cl₂, **2**·2CHCl₃, **3**·4MeCN, and **4**

	1	2	3	4
formula[a]	C₆₀H₅₉Cl₂Fe₅N₂O₂₁	C₆₂H₁₁₆Cl₆Fe₆N₄O₂₆	C₆₀H₁₁₆Cl₄Fe₁₂N₁₂O₅₂	C₄₀H₉₂Cl₄Fe₁₂N₈O₄₆
fw, g/mol[a]	1494.27	1881.39	2649.61	2233.17
space group	P2₁/c	C2/c	C2/c	C2/c
a, Å	21.3735(10)	14.211(2)	29.590(4)	30.502(3)
b, Å	18.6612(9)	24.297(2)	29.641(4)	11.9702(11)
c, Å	17.7842(8)	25.676(3)	23.174(3)	30.517(3)
α, °	90	90	90	90
β, °	113.280(1)	94.783(3)	104.088(2)	111.404(1)
γ, °	90	90	90	90
V, Å³	6515.81	8988.6(15)	19714(5)	10373.7
Z	4	4	8	4
T, K	173(2)	173(2)	173(2)	173(2)
radiation, Å[b]	0.71073	0.71073	0.71073	0.71073
ρ_calc, g/cm³		1.414	1.764	
μ, mm⁻¹		1.210	1.916	
R1[c,d]		0.0575	0.0788	
wR2[e]		0.1364	0.2219	

[a] Including solvate molecules. [b] Graphite monochromator. [c] $I > 2\sigma(I)$. [d] $R1 = \Sigma(\triangle|F_o| - |F_c\triangle|)/\Sigma|F_o|$. [e] $wR2 = [\Sigma[w(F_o^2 - F_c^2)^2]/\Sigma[w(F_o^2)^2]]^{1/2}$, $w = 1/[\sigma^2(F_o^2) + [(ap)^2 + bp]$, where $p = [\max (F_o^2, O) + 2F_c^2]/3$.
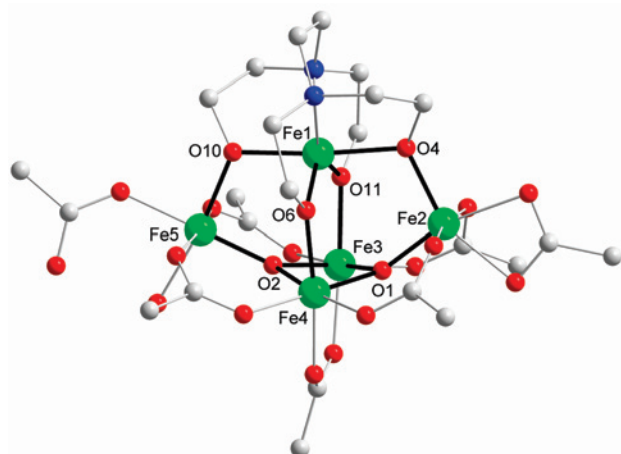
Figure 1. Labeled representation of the partially refined structure of **1** with core Fe−O bonds as thick black lines; only the ipso benzoate carbon atoms are shown. Color code: Fe, green; O, red; N, blue; C, grey.

Complex **1** crystallizes in the monoclinic space group $P2_1/c$ and consists of an $[Fe_4(\mu_3\text{-}O)_2]^{8+}$ butterfly like subunit (Fe2, Fe3, Fe4, and Fe5) on the top of which is attached an $[Fe(\mu\text{-}OR)_4]$ unit containing Fe1. There is an O atom monoatomically bridging Fe1 to each of the four Fe atoms of the butterfly. These four O atoms (O4, O6, O10, and O11) are the alkoxide arms of the edte^{4-} group, which is hexadentate with its four deprotonated alkoxide O atoms all adopting μ-bridging modes; thus, the edte^{4-} group is overall μ_5, as shown in Figure 2a. Peripheral ligation about the core is provided by one water molecule on Fe5 and seven benzoates, out of which five are in $\eta^1:\eta^1:\mu$- bridging mode, one is η^1 terminal on Fe5, and one is η^2 chelating on Fe2. There are relatively few Fe$_5$ clusters reported in the literature, and these have Fe$_5$ topologies such as a square pyramid, a centered tetrahedron, and a partial cubane extended at one face by a partial adamantane unit.[12] However, the only previous compound with an $[Fe_5O_6]$ core structurally similar to that in **1** is $[Fe_5O_2(OH)(O_2CMe)_5(hmbp)_3]^{2+}$ (**6**; hmbpH = 6-hydroxymethyl-2,2′-bipyridine).[13]

The labeled structure of $[Fe_6O_2(O_2CBu^t)_8(edteH)_2]$ (**2**) is shown in Figure 3. Selected interatomic distances and angles are summarized in Table 2. Complex **2** crystallizes in the monoclinic space group $C2/c$. The centrosymmetric structure consists of a roughly planar arrangement of six Fe(III) atoms consisting of two triangular $[Fe_3(\mu_3\text{-}O)]^{7+}$ units joined together by four alkoxide edte O atoms, O4 and O13. Each triangular unit is essentially isosceles (Fe1⋯Fe2 = 2.986

(12) (a) Tabernor, J.; Jones, L. F.; Heath, S. L.; Muryn, C.; Aromi, G.; Ribas, J.; Brechin, E. K.; Collison, D. *Dalton Trans.* **2004**, 975. (b) Boskovic, C.; Sieber, A.; Chaboussant, G.; Guedel, H. U.; Ensling, J.; Wernsdorfer, W.; Neels, A.; Labat, G.; Stoeckli-Evans, H.; Janssen, S. *Inorg. Chem.* **2004**, *43*, 5053. (c) Boskovic, C.; Labat, G.; Neels, A.; Gudel, H. U. *Dalton Trans.* **2003**, 3671. (d) Lachicotte, R. J.; Hagen, K. S. *Inorg. Chim. Acta* **1997**, *263*, 407. (e) Reynolds, R. A.; Coucouvanis, D. *Inorg. Chem.* **1998**, *37*, 170. (f) O'Keefe, B. J.; Monnier, S. M.; Hillmyer, M. A.; Tolman, W. B. *J. Am. Chem. Soc.* **2001**, *123*, 339. (g) Mikuriya, M.; Nakadera, K. *Chem. Lett.* **1995**, *3*, 213. (h) Mikuriya, M.; Hashimoto, Y.; Nakashima, S. *Chem. Commun.* **1996**, 295. (j) Herold, S.; Lippard, S. J. *Inorg. Chem.* **1997**, *36*, 50. (k) Krishnamurthy, D.; Sarjeant, A. N.; Goldberg, D. P.; Caneschi, A.; Totti, F.; Zakharov, L. N.; Rheingold, A. L. *Chem.−Eur. J.* **2005**, *11*, 7328.
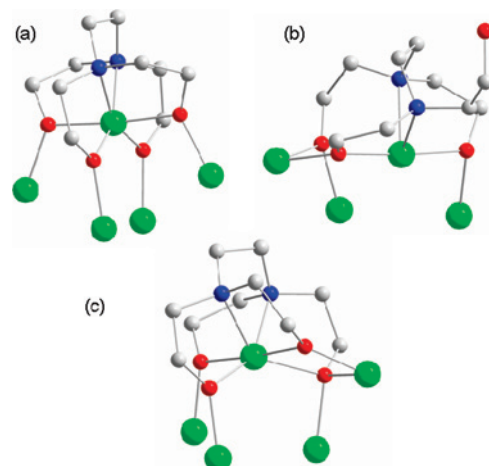(13) Bagai, R.; Abboud, K. A.; Christou, G. *Inorg. Chem.* **2007**, *46*, 5567.

Figure 2. Crystallographically established coordination modes of edte^{4-} and edteH^{3-} in complexes **1−3**. Color code: Fe, green; O, red; N, blue; C, grey.
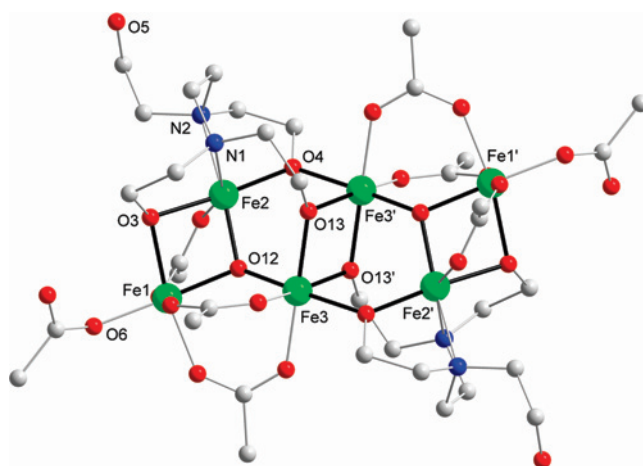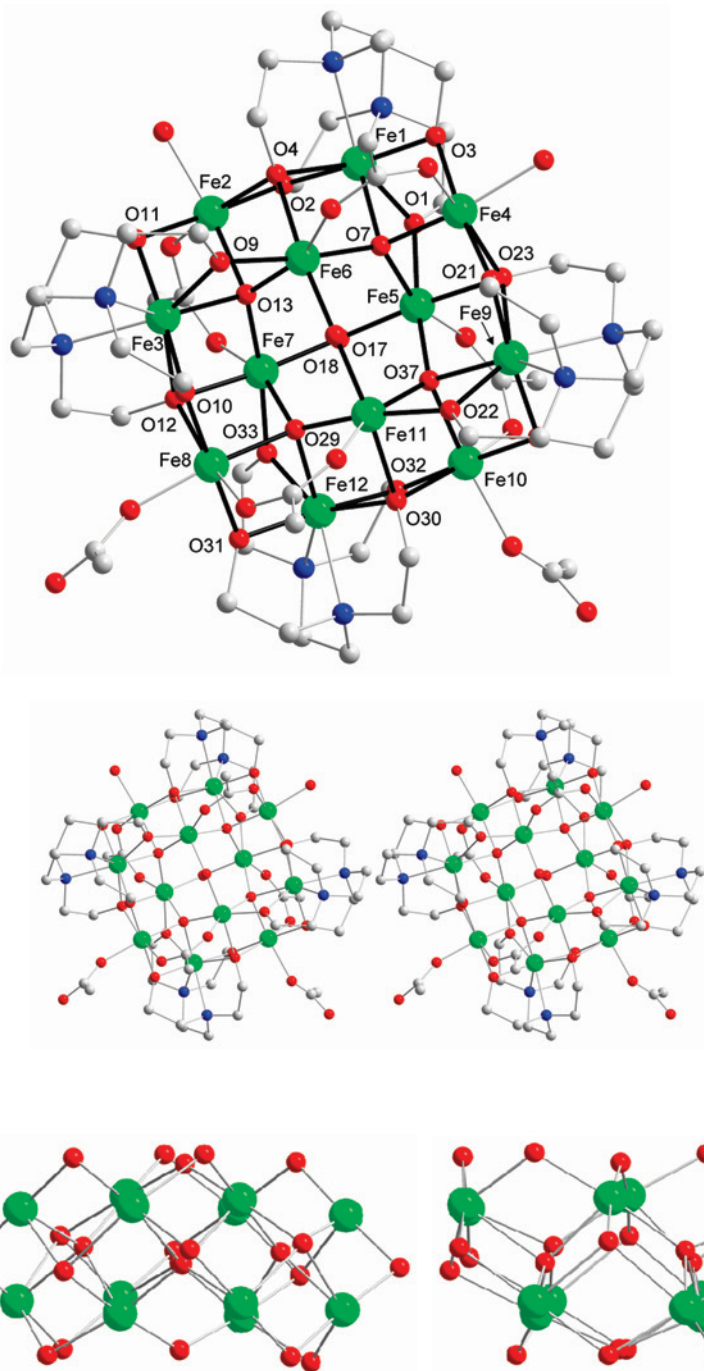

Figure 3. Labeled representation of the structure of **2** with core Fe−O bonds as thick black lines; pivalate Me groups have been omitted for clarity. Color code: Fe, green; O, red; N, blue; C, grey.

Table 2. Selected Bond Distances (Å) and Angles (°) for **2·2CHCl$_3$**

Fe1−O12	1.931(2)	Fe2−O2	2.050(3)
Fe1−O6	1.957(3)	Fe2−N2	2.251(3)
Fe1−O10	2.025(3)	Fe2−N1	2.289(3)
Fe1−O8	2.026(3)	Fe3−O12	1.858(2)
Fe1−O1	2.037(3)	Fe3−O13′	2.019(3)
Fe1−O3	2.051(2)	Fe3−O13	2.033(2)
Fe2−O12	1.907(2)	Fe3−O4′	2.034(2)
Fe2−O4	1.965(3)	Fe3−O11	2.039(3)
Fe2−O3	2.030(3)	Fe3−O9	2.040(3)
Fe3−O12−Fe2	123.25(13)	Fe3′−O13−Fe3	102.33(11)
Fe3−O12−Fe1	123.83(13)	Fe2−O3−Fe1	94.06(10)
Fe2−O12−Fe1	102.16(11)	Fe2−O4−Fe3′	118.77(12)

Å, Fe2⋯Fe3 = 3.313 Å, Fe1⋯Fe3 = 3.344 Å) with the oxide (atom O12) 0.359 Å out of the Fe$_3$ plane. All the Fe atoms are six-coordinate. The two edteH^{3-} groups are η^4-chelating on Fe2 and Fe2′, with their three deprotonated alkoxide arms (O3, O4, O13) each bridging a separate Fe$_2$ pair, and the protonated alcohol arm (O5) unbound. Each edteH^{3-} group is thus overall μ_4, as shown in Figure 2b. The peripheral ligation is provided by eight pivalate groups, of which six are $\eta^1:\eta^1:\mu$-bridging and two are η^1 terminal on Fe1 and Fe1′. The bond-valence sums (BVS)[14] for the O atoms of edteH^{3-} are listed in the (Supporting Information Table S1), confirming the triply deprotonated description.

Figure 4. (top) Labeled representation of the cation of **3** with core Fe−O bonds as thick black lines; (middle) a stereopair; (bottom) side-views of the core, emphasizing the layered structure. Color code: Fe, green; O, red; N, blue; C, grey.

The protonated oxygen atom, O5, is involved in intermolecular H-bonding to pivalate atom O1 of an adjacent molecule forming one-dimensional chains running in two directions in the crystal.

The core of complex **2** is unprecedented in hexanuclear Fe(III) chemistry. A number of Fe₆ clusters have been reported in the literature, and a recent listing of these, together with their structural types, is available elsewhere.[15] Among these are a family of Fe₆ clusters whose cores comprise

linked $[Fe_3(\mu_3\text{-}O)]^{7+}$ triangular subunits as in **2**, but the two units are bridged by multiple hydroxo or alkoxo groups; overall, all these prior complexes possess core structures different from that of the present complex **2**.

The labeled structure of the cation of $[Fe_{12}O_4(OH)_2(O_2CMe)_6$-$(edte)_4(H_2O)_2](ClO_4)_4$ (**3**) is shown in Figure 4, and selected interatomic distances and angles are listed in Table 3. Complex **3** crystallizes in the monoclinic space group *C*2/*c*. The structure consists of an $[Fe^{III}_{12}(\mu_4\text{-}O)_4(\mu\text{-}OH)_2(\mu\text{-}$

(14) Brown, I. D.; Altermatt, D. *Acta Crystallogr., Sect. B: Struct. Sci.* **1985**, *B41*, 244.

(15) Taguchi, T.; Stamatatos, T. C.; Abboud, K. A.; Jones, C. M.; O'Brien, T. A.; Christou, G. Inorg. Chem. 2008, in press.

Table 3. Selected Bond Distances (Å) and Angles (°) for **3·4MeCN**

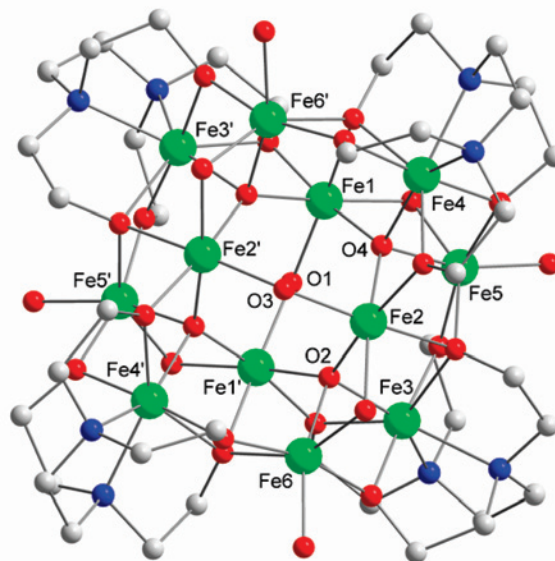|			
Fe1−O2	1.977(6)	Fe6−O4	2.074(6)
Fe1−O3	1.985(6)	Fe7−O17	1.926(6)
Fe1−O1	2.040(6)	Fe7−O33	1.969(6)
Fe1−O7	2.187(6)	Fe7−O13	1.982(6)
Fe1−O4	2.223(6)	Fe7−O29	2.037(6)
Fe2−O2	1.964(6)	Fe7−O12	2.092(6)
Fe2−O11	1.984(7)	Fe8−O19	1.972(7)
Fe2−O5	2.010(7)	Fe8−O10	1.976(7)
Fe2−O13	2.053(6)	Fe8−O31	2.001(7)
Fe2−O4	2.104(6)	Fe8−O29	2.068(6)
Fe3−O10	1.972(7)	Fe8−O12	2.098(6)
Fe3−O11	1.988(7)	Fe9−O21	1.959(6)
Fe3−O9	2.038(6)	Fe9−O24	1.979(6)
Fe3−O13	2.160(6)	Fe9−O22	2.031(7)
Fe3−O12	2.239(6)	Fe9−O37	2.186(6)
Fe4−O3	1.975(6)	Fe9−O23	2.237(7)
Fe4−O21	1.981(7)	Fe10−O32	1.954(6)
Fe4−O7	2.004(6)	Fe10−O24	1.974(6)
Fe4−O16	2.080(6)	Fe10−O26	1.995(8)
Fe4−O23	2.098(6)	Fe10−O37	2.031(6)
Fe5−O17	1.944(6)	Fe10−O27	2.032(7)
Fe5−O1	1.968(7)	Fe10−O30	2.103(7)
Fe5−O37	1.971(6)	Fe11−O18	1.952(6)
Fe5−O7	2.032(6)	Fe11−O29	1.963(6)
Fe5−O23	2.104(6)	Fe11−O22	1.980(6)
Fe6−O18	1.939(6)	Fe11−O37	2.026(6)
Fe6−O9	1.967(6)	Fe11−O30	2.093(6)
Fe6−O7	1.980(6)	Fe12−O32	1.962(6)
Fe6−O13	2.013(6)	Fe12−O31	1.976(7)
Fe12−O29	2.156(6)	Fe12−O30	2.236(7)
Fe7−O17−Fe5	135.1(3)	Fe6−O18−Fe11	134.1(3)

Figure 5. Labeled representation of the partially refined structure of the cation of **4** with core Fe−O bonds as thick black lines. Color code: Fe, green; O, red; N, blue; C, grey.

$O_2CMe)_4(\mu_3\text{-}OR)_4(\mu\text{-}OR)_{12}]^{2+}$ core consisting of two near-planar Fe_6 layers sandwiched between three near-planar layers of O atoms (Figure 4, bottom). All the Fe atoms are six-coordinate except Fe1, Fe3, Fe9, and Fe12, which are seven-coordinate. The four $\mu_4\text{-}O^{2-}$ ions (O7, O13, O29, and O37) together serve to connect all twelve Fe atoms. Each edte^{4-} group is hexadentate-chelating on Fe atoms Fe1, Fe3, Fe9, and Fe12, with each of its deprotonated alkoxide arms bridging to either one or two additional Fe atoms. Thus, the edte^{4-} groups are overall μ_5, as shown in Figure 2c. The protonation levels of the O^{2-}, OH^-, and OR^- groups were determined from a combination of charge balance considerations, inspection of bond lengths, and BVS calculations (Supporting Information Table S1). The edte^{4-} O atoms have BVS values of >1.87, confirming them as completely deprotonated, as concluded above from their bridging modes. In contrast, O17 and O18 have a BVS of 1.24 and 1.20 as expected for an OH^- group. Peripheral ligation is provided by two terminal water molecules and six acetate groups, of which four are $\eta^1:\eta^1:\mu$ bridging and two are η^1 terminal on Fe8 and Fe10.

Complex **3** is only one of a very few dodecanuclear Fe(III) clusters in the literature, of which the majority have a wheel or loop structure.[16] Among the remainder, one is composed of face-sharing defect cuboidal units in the central fragment

of the core, and the other consists of four edge sharing $[Fe_3(\mu_3\text{-}O)]^{7+}$ units.[17] The structure of complex **3** is thus unprecedented in Fe chemistry but is similar to that recently reported in Mn chemistry with a formula $[Mn_{12}O_4(OH)_2(edte)_4\text{-}Cl_6(H_2O)_2]$ and a mixed-valence $Mn^{III}_8Mn^{II}_4$ description.[6]

The labeled structure of the cation of $[Fe_{12}O_4(OH)_8(edte)_4\text{-}(H_2O)_2](ClO_4)_4$ (**4**) is shown in Figure 5. The core is essentially the same as that of **3** except that acetate groups have been replaced by hydroxide ones. Complex **5** gave an elemental analysis consistent with it being the NO_3^- salt of the same cation as **4** and is thus formulated as $[Fe_{12}O_4\text{-}(OH)_8(edte)_4(H_2O)_2](NO_3)_4$. This conclusion is also supported by the very similar magnetic properties of **4** and **5** (vide infra) and, indeed, the very similar magnetic properties of all three complexes **3**−**5**, which is consistent with the conclusion that they all possess the same or very similar Fe_{12} core structure.

Magnetochemistry. Solid-state, variable-temperature dc magnetic susceptibility data were collected in a 0.1 T field and in the 5.0–300 K range on powdered crystalline samples of **1**−**5** restrained in eicosane. The obtained data are plotted as $\chi_M T$ versus T in Figure 6. For **1**, $\chi_M T$ steadily decreases from 6.73 cm^3 K mol^{-1} at 300 K to 3.88 cm^3 K mol^{-1} at 40.0 K, then stays approximately constant until 25.0 K, and increases slightly to 4.02 cm^3 K mol^{-1} at 5.0 K. The 300 K value is much less than the spin-only ($g = 2$) value of 21.87 cm^3 K mol^{-1} for five noninteracting Fe(III) atoms, indicating the presence of strong antiferromagnetic interactions, as expected for oxo-bridged Fe(III) systems. The 5.0 K value of 4.02 cm^3 K mol^{-1} suggests an $S = 5/2$ ground-state spin. $\chi_M T$ for **2·2CHCl$_3$·4H$_2$O** is 11.03 cm^3 K mol^{-1} at 300 K, stays approximately constant with decreasing temperature to 100 K, and then increases to 13.83 cm^3 K mol^{-1} at 5 K. $\chi_M T$ at 300 K is again much less than the spin-only value of

(16) (a) Abu-Nawwas, A. A. H.; Cano, J.; Christian, P.; Mallah, T.; Rajaraman, G.; Teat, S. J.; Winpenny, R. E. P.; Yukawa, Y. *Chem. Commun.* **2004**, 314. (b) Sellmann, D.; Geipel, F.; Heinemann, F. W. *Chem.—Eur. J.* **2002**, *8*, 958. (c) Caneschi, A.; Cornia, A.; Fabretti, A. C.; Gatteschi, D. *Angew. Chem., Int. Ed.* **1999**, *38*, 1295. (d) Schmitt, W.; Anson, C. E.; Pilawa, B.; Powell, A. K. *Z. Anorg. Allg. Chem.* **2002**, *628*, 2443. (e) Raptopoulou, C. P.; Tangoulis, V.; Devlin, E. *Angew. Chem., Int. Ed.* **2002**, *41*, 2386. (f) Stamatatos, T. C.; Christou, A. G.; Jones, C. M.; O'Callaghan, B. J.; Abboud, K. A.; O'Brien, T. A.; Christou, G. *J. Am. Chem. Soc.* **2007**, *129*, 9840.

(17) (a) Murugesu, M.; Abboud, K. A.; Christou, G. *Polyhedron* **2004**, *23*, 2779. (b) Boskovic, C.; Gudel, H. U.; Labat, G.; Neels, A.; Wernsdorfer, W.; Moubaraki, B.; Murray, K. S. *Inorg. Chem.* **2005**, *44*, 3181.
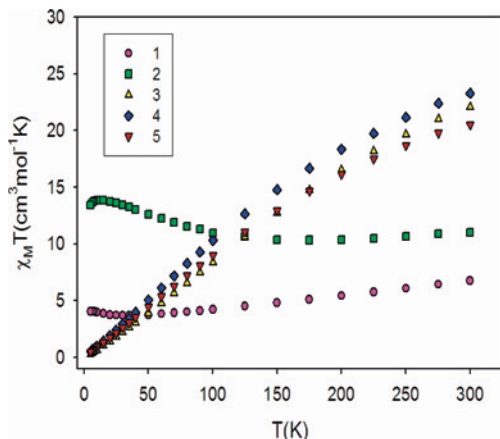
Figure 6. Plots of dc $\chi_M T$ versus T for complexes **1−5**.

26.25 cm³ K mol⁻¹ expected for six noninteracting Fe(III) ions, indicating strong antiferromagnetic interactions. The 5.0 K value of 13.83 cm³ K mol⁻¹ suggests an $S = 5$ ground-state spin.

The $\chi_M T$ versus T plots for the three complexes **3−5** in Figure 6 are very similar, indicating a minimal influence of the peripheral groups and supporting the conclusions above that they possess similar core structures. For **3−5**, $\chi_M T$ steadily decreases from 22.04, 23.37, 20.53 cm³ K mol⁻¹ at 300 K to 0.25, 0.51, 0.50 cm³ K mol⁻¹ at 5.0 K, respectively. The change in $\chi_M T$ with decreasing temperature and the low value at 5 K are indicative of an $S = 0$ ground state. The differences in $\chi_M T$ versus T for the three complexes are almost certainly just reflecting small differences in intramolecular exchange coupling constants (J) and perhaps in zero-field splitting (ZFS) parameters (D) and any intermolecular interactions.

To confirm the initial ground-state spin estimates above for **1** and **2**, variable-field (H) and -temperature magnetization (M) data were collected in the 0.1–7.0 T and 1.8–10 K ranges. The resulting data for **1** are plotted in Figure 7 (top) as reduced magnetization ($M/N\mu_B$) versus H/T, where N is Avogadro's number and μ_B is the Bohr magneton. The saturation value at the highest fields and lowest temperatures is ~4.90, as expected for an $S = 5/2$ ground state, and g slightly less than 2; the saturation value should be gS in the absence of complications from low-lying excited states. The data were fit, using the program MAGNET[10] by diagonalization of the spin Hamiltonian matrix assuming only the ground state is populated, incorporating axial anisotropy ($D\hat{S}_z^2$) and the Zeeman interaction, and employing a full powder average. The corresponding spin Hamiltonian is given by eq 4, where $\hat{S}_z$ is the z-axis spin operator, g is the electronic g factor, μ_0

$$\mathbf{H} = D\hat{S}_z^2 + g\mu_B\mu_0\hat{S}\cdot H \quad (4)$$

is the vacuum permeability, and H is the applied field. The last term in eq 4 is the Zeeman energy associated with an applied magnetic field. The best fit for **1** is shown as the solid lines in Figure 7 (top) and was obtained with $S = 5/2$ and either of the two sets of parameters: $g = 1.96$ and $D = 0.58$ cm⁻¹, and $g = 1.96$ and $D = -0.50$ cm⁻¹. Alternative fits with $S = 3/2$ or $7/2$ were rejected because they gave
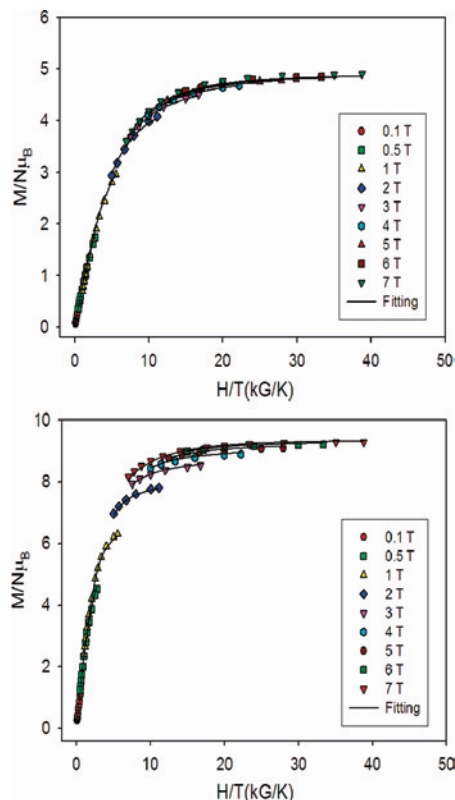

Figure 7. Plot of reduced magnetization ($M/N\mu_B$) vs H/T for complexes **1** (top) and **2·2CHCl₃·4H₂O** (bottom). The solid lines are the fits of the data; see the text for the fit parameters.

unreasonable values of g and D. It is common to obtain two acceptable fits of magnetization data for a given S value, one with $D > 0$ and the other with $D < 0$, since magnetization fits are not very sensitive to the sign of D. This was indeed the case for the magnetization fits for both the complexes **1** and **2**. To assess which is the superior fit for these complexes and also to ensure that the true global minimum had been located in each case, we calculated the root-mean-square error surface for the fits as a function of D and g using the program GRID,[18] which calculates the relative difference between the experimental $M/N\mu_B$ data and those calculated for various combinations of D and g. For **1**, the error surface (Supporting Information Figure S1) clearly shows the two minima with positive and negative D values, with the fit with negative D being clearly superior and suggesting that this is the true sign of D. However, it would require a more sensitive technique such as electron paramagnetic resonance spectroscopy to confirm this.

The obtained magnetization data for **2** are plotted in Figure 7 (bottom) as $M/N\mu_B$ versus H/T, and it can be seen to saturate at ~9.29, suggesting an $S = 5$ ground state and $g < 2$. The resulting best fits of the data are shown as the solid lines in Figure 7 (bottom) and were obtained with $S = 5$ and either $g = 1.90$, $D = 0.45$ cm⁻¹ or $g = 1.89$, $D = -0.28$ cm⁻¹. In this case also, the fit error surface (Supporting Information Figure S2) clearly shows that the fit with negative D is far superior, suggesting this to be the true sign of D.

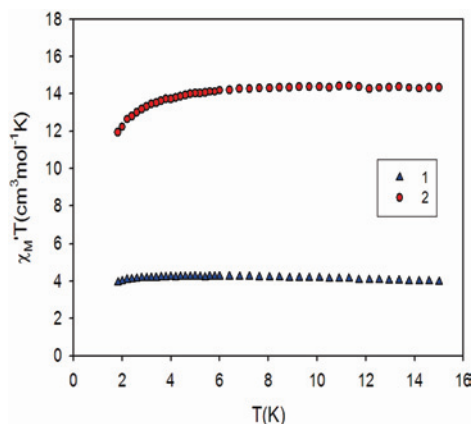(18) Davidson, E. R. *GRID*; Indiana University: Bloomington, IN, 1999.

Figure 8. In-phase ac magnetic susceptibility signals at 997 Hz for complexes **1** and **2** confirming them as possessing $S = 5/2$ and 5 ground states, respectively.
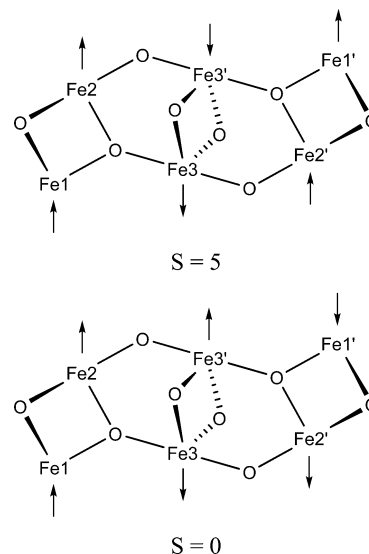

Figure 9. (top) Spin alignments at the six $S = 5/2$ Fe(III) atoms of **2** rationalizing its overall $S = 5$ ground state, based on the arguments given in the text. (bottom) Spin alignments if the strengths of the Fe2/Fe3′ and Fe3/Fe3′ couplings were reversed, showing that the wrong ground state would be obtained.

The magnetization fits confirmed the preliminary estimates of the ground-state spin S of **1** and **2**, but we nevertheless sought an additional and independent means of confirmation. This was accomplished using ac susceptibility data collected on microcrystalline samples in a 3.5 G ac field. The in-phase (χ_M') ac susceptibility signal is invaluable for assessing S without any complications from a dc field,[19] and these signals for complexes **1** and **2** at 997 Hz are plotted as $\chi_M'T$ versus T in Figure 8. The $\chi_M'T$ is essentially temperature independent below 15 K until ~4–5 K where there is a small decrease that can be assigned to low temperature effects such as ZFS of the ground state and/or very weak intermolecular interactions. The essentially constant values at >5 K of ~4 and ~14 cm³ K mol⁻¹ for **1** and **2**, respectively, confirm $S = 5/2$ and 5 ground states with $g < 2$, whose spin-only ($g = 2.0$) values are 4.38 and 15.0 cm³ K mol⁻¹, respectively. Neither complex displayed out-of-phase (χ_M'') ac susceptibility peaks above 1.8 K.

Rationalization of the Observed Ground State S Values. It is of interest to attempt to rationalize the observed ground-state spin values of **1** and **2**. It is assumed that all Fe₂ pairwise exchange interactions are antiferromagnetic, as is essentially always the case for high-spin Fe(III), and there will thus be competing antiferromagnetic exchange interactions and spin frustration effects within the many Fe₃ triangular units in these complexes. In fact, for complex **1**, its $S = 5/2$ ground state can be rationalized in an identical fashion, based on spin frustration, as we previously described for complex **6**, which has a similar [Fe₅O₆] core topology as **1**, as stated earlier, and an identical $S = 5/2$ ground state.[13]

For complex **2**, the spin alignments giving rise to the $S = 5$ ground state are again not obvious owing to spin frustration within the triangular units of the Fe₆ core. There are five inequivalent types of exchange interactions, J_{12}, J_{13}, J_{23}, $J_{23'}$ and $J_{33'}$, the subscripts referring to the atom labels of Figure 3. In Table 4, we list the average Fe−O distances and the

Fe−O−Fe angles for bridged Fe₂ pairs within the molecule. It is well-known that short Fe−O bond distances and large Fe−O−Fe angles lead to the larger J values.[20,21] In complex **2**, the Fe1/Fe3 and Fe2/Fe3 pairs, with only a single monatomic bridge, have both the shortest Fe−O superexchange pathways and the largest Fe−O−Fe angles in the molecule and are thus expected on the basis of magneto-structural correlations[20] to have the strongest J values, in the order of ~40 cm⁻¹. The Fe2/Fe3′ pair, also with a single monatomic bridge, has a slightly longer Fe−O pathway but still a large Fe−O−Fe angle; thus, it would also be expected to have a relatively strong J value, in the ~15 cm⁻¹ region. In contrast, the Fe1/Fe2 and Fe3/Fe3′ pairs, which are now bis-monatomically bridged, have Fe−O distances similar to that for Fe2/Fe3′ but by far the smallest Fe−O−Fe angles in the molecule and would thus be expected to have the weakest J values, in the ~7 cm⁻¹ region. The estimates given are based on the J values predicted for Fe₂ pairs with similar metric parameters in magnetostructural correlations derived from other Fe(III) clusters.[21] Thus, we conclude that the Fe1/Fe2 and Fe3/Fe3′ exchange will be frustrated by the other, stronger interactions, and as a result, the ground-state spin alignments in the molecule will be as shown in Figure 9 (top). The spins within the Fe₂ pairs monatomically bridged by a single O atom are aligned antiparallel, whereas those within the three bis-monatomically bridged Fe₂ pairs are spin frustrated by the other stronger interactions and forced to align parallel even though their exchange interactions are intrinsically antiferromagnetic. This situation predicts an $S = 5$ ground state for **2**, as experimentally obtained. Note that it is not easy to formulate other reasonable ways of

(19) (a) Brechin, E. K.; Sanudo, E. C.; Wernsdorfer, W.; Boskovic, C.; Yoo, J.; Hendrickson, D. N.; Yamaguchi, A.; Ishimoto, H.; Concolino, T. E.; Rheingold, A. L.; Christou, G. *Inorg. Chem.* **2005**, *44*, 502. (b) Sanudo, E. C.; Wernsdorfer, W.; Abboud, K. A.; Christou, G. *Inorg. Chem.* **2004**, *43*, 4137. (c) Murugesu, M.; Habrych, M.; Wernsdorfer, W.; Abboud, K. A.; Christou, G. *J. Am. Chem. Soc.* **2004**, *126*, 4766.

(20) (a) Weihe, H.; Gudel, H. U. *J. Am. Chem. Soc.* **1997**, *119*, 6539. (b) Werner, R.; Ostrovsky, S.; Griesar, K.; Haase, W. *Inorg. Chim. Acta* **2001**, *326*, 78. (c) Gorun, S. M.; Lippard, S. J. *Inorg. Chem.* **1991**, *30*, 1625.

(21) Canada-Vilalta, C.; O'Brien, T. A.; Brechin, E. K.; Pink, M.; Davidson, E. R.; Christou, G. *Inorg. Chem.* **2004**, *43*, 5505.

Table 4. Selected Fe−O Distances and Fe−O−Fe Angles for **2**

Fe₂ pair	avg. Fe−O (Å)	angle (deg)	estimated J
Fe1/Fe3	1.895	123.8	$\sim-40 \mathrm{cm}^{-1}$
Fe2/Fe3	1.883	123.2	$\sim-40 \mathrm{cm}^{-1}$
Fe2/Fe3′	2.000	118.7	$\sim-15 \mathrm{cm}^{-1}$
Fe3/Fe3′	2.026	102.3	$\sim-7 \mathrm{cm}^{-1}$
Fe1/Fe2	1.980	98.1 (avg.)	$\sim-7 \mathrm{cm}^{-1}$

getting an $S = 5$ ground state. For example, if the Fe2/Fe3′ interaction were considerably weaker, enough to be frustrated by the Fe3/Fe3′ interaction, then this situation would give the spin alignments of Figure 9 (bottom) and an $S = 0$ ground state.

It is difficult to rationalize the $S = 0$ ground-state spin for **3** because of the high content of triangular units and the large number of nonzero exchange interactions. Even assuming virtual $S4$ symmetry, there are too many nonequivalent J values within the molecule to allow a meaningful rationalization of the $S = 0$ ground state.

Conclusions

The initial use of edteH₄ in Fe cluster chemistry has provided an entry into Fe₅, Fe₆, and Fe₁₂ cluster types. This supports our original suspicion that the polyfunctional edteH₄ molecule could, on partial or complete deprotonation, act as an excellent bridging ligand of multiple Fe atoms and thus foster formation of high nuclearity products. Although the core of complex **1** is overall similar to that of a previous Fe₅ complex with hmbp⁻, those of the Fe₆ complex **2** and particularly that of the Fe₁₂ complex **3** are unprecedented in Fe(III) chemistry. We were frustrated in our attempts to better characterize the structure of the analogous complex **4**, but we could at least confirm the same overall Fe₁₂ topology as seen in **3**. The structures of the cations **4** and **5** are concluded to be the same given their identical formulations and almost superimposable magnetic properties. We have also successfully rationalized the $S = 5$ ground state of **2** using simple ideas of spin frustration and estimates of the various J values from available magnetostructural correlations. The combined results described emphasize the usefulness of the poly alcohol-based chelate edteH₄ as a route to new high-nuclearity products. Thus, several additional directions employing this chelate are currently in progress, including with other metals, and will be reported in due course.

Supporting Information Available: X-ray crystallographic data in CIF format for complex **2**·2CHCl₃ and **3**·4MeCN; BVS sums for O atoms of complex **2** and **3**; and two-dimensional contour plots of the rms error surfaces vs D and g for the magnetization fits for **1** and **2**·2CHCl₃·4H₂O (PDF). This material is available free of charge via the Internet at http://pubs.acs.org.

IC7024022